RADIO EMISSION AND ATMOSPHERIC STRUCTURE ABOVE SUNSPOTS

M. A. Livshits, V. N. Obridko, and S. B. Pikel'ner

Institute of Terrestrial Magnetism, the Ionosphere, and Radio-Wave Propagation, Academy of Sciences of the USSR
Shternberg Astronomical Institute, Moscow

Translated from Astronomicheskii Zhurnal, Vol. 43, No. 6, pp. 1135-1142, November-December, 1966
Original article submitted March 22, 1966

The circularly polarized magnetobremsstrahlung at centimeter wavelengths from regions above sunspots requires a field $H \approx 1000$ Oe and a coronal temperature $\approx 10^6$ °K. Direct observations of photospheric and chromospheric fields and theoretical indications for strong broadening of the magnetic tube of force in rarefied atmospheric layers imply that $H \approx 1000$ Oe only below 3000-km height. Thus the corona evidently begins at a small height above spots. A model radio source is computed from observed radio spectra and information on circular polarization. A hydrostatic density distribution is assumed. The radio data furnish a fairly reliable $T(h)$ curve. A natural explanation is also obtained for the directivity of the radiation, the sharp source boundary, and the correspondence between sources and spot umbrae. The chromosphere above spots differs from the ordinary chromosphere because of the poor dissipation of Alfvén and accelerated waves in a strong field. Retarded (sound) waves decay low in the chromosphere, generating no appreciable heating. Apparently only accelerated waves can penetrate the corona, where they are transformed into other types of wave and decay at a great height. Energy is thence transported by heat conduction into the low coronal layers responsible for the radio emission.

1. Height of Radio Sources above Sunspots

Observations during eclipse and with high-resolution radio telescopes have revealed that the sources of the slowly varying component of radio emission are related to active formations on the solar surface. Within the wavelength range 1-10 cm the source consists of a nucleus, of sunspot size ($\approx 1'$) and with a brightness temperature $T \approx 10^6$ °K, and a halo above the active region with a diameter of $\approx 5'$ and $T \leqslant 10^5$ °K. The lifetime of the source above a spot agrees with the spot lifetime.

The spectra of sources above spots exhibit considerable variety [1-3], but in all cases the energy flux rises from $\lambda = 3$ cm to $\lambda = 5$ cm. The flux reaches a maximum at $\lambda = 5$-10 cm [1-3]. The radiation is partially circularly polarized, with the degree of polarization increasing from ≈10% at $\lambda = 10$ cm to 30% or more at $\leqslant 3$ cm. The direction of rotation corresponds to emergence of the extraordinary wave from the spot field. The size of the sources in polarized light agrees with that of spot umbrae [4]. The radiation is directional, with the flux varying as $\cos\theta$ at the longer wavelengths. From the displacement of the center of the radio-emitting region relative to spots, different authors have obtained different heights, in many cases exceeding 20,000 km [5, 6]. However, these measurements demand very high resolving power and possess low accuracy.

The intensity, spectrum, and polarization of the radio emission above spots can be explained only through the magnetobremsstrahlung mechanism [5, 7]. The absorption coefficient of the extraordinary wave increases sharply for the har-

monics of the gyrofrequency. Hence the brightness of this wave is determined by the half of the Planck function for the temperature of the layer, where the second and third harmonics of the gyrofrequency correspond to the frequency received.

In order for this mechanism to explain the radiation at 3-6 cm, gas at a temperature $> 10^6$ °K must be subject to a magnetic field $H \approx 1000$ Oe. So high a field strength is apparently inadmissible at coronal height ($\gtrsim 20{,}000$ km). Indeed, at the photospheric level $H \approx 3000$-4000 Oe in large spots. However, even the earliest measurements of the height dependence of the field revealed a fairly sharp decline in the field strength: $dH_\parallel/dh \approx -0.5$ to -1 Oe/km [8-10]. Direct measurements of the field above spots yield for the $H\alpha$ and $H\beta$ lines (heights 1000-3000 km) the values $H \approx 1000$-1500 Oe [10, 11]. Detailed studies of the total H vector in spots, as carried out in the past few years both photographically [12, 13] and with a magnetograph [14, 15], have shown that at the photospheric level the lines of force diverge quite rapidly from the spot axis. The field gradient $dH_\parallel/dh \approx -0.5$ Oe/km has been computed from the divergence of the lines of force (div $H = 0$) [14, 15]. Thus various observers have found a rapid decline in intensity with height. From a theoretical standpoint it would also be very difficult to believe that any substantial part of the magnetic flux of a spot could rise to a height $\gtrsim 20{,}000$ km without appreciable broadening because of magnetic pressure. In the rarefied chromosphere there are in fact no forces that could contain a narrow tube with a field $H \approx 1000$ Oe. For quantitative estimates we may use the fact that the accumulated observations of spot fields can be represented approximately by a dipole submerged 10,000-15,000 km beneath the photosphere [15]. The dipole component should naturally be the basic one for the bundle of lines of force emerging from beneath the photosphere surface. With this representation the value $H \approx 1000$ Oe would be reached at heights of 2000-3000 km.

If we adopt the magnetobremsstrahlung mechanism to explain the radio emission above spots, we would then suppose that regions of coronal temperature sink to these low heights above spots. So unusual an assumption would of course conflict with the radio-source height determinations mentioned above. Nevertheless, these determinations were made with low resolving power and hence are subject to large error. Moreover, in some cases the same measurements yield a considerably smaller height [2]. The rise of a radio source from behind the limb usually leads the appearance of the spot by about one day, but the low surface temperature and apparently the weak polarization imply that the emission is related not to magnetobremsstrahlung but simply to bremsstrahlung from the overlying coronal regions above the spots (coronal condensation). Polarization measurements secured during the 1958 eclipse yielded a height of ≈35,000 km [4]. However, a careful comparison of the radio-emitting regions with optical photospheric observations that were made at the Pulkovo Observatory has shown that the regions of polarized radiation coincided very accurately with the position of the spot umbrae. This result indicates that the heights have small values (G. B. Gel'freikh and R. S. Gnevysheva).

An analysis of the radio sources compels us, then, to conclude that the corona sets in at a height of 2000-3000 km above spots. As will be shown below, this configuration would provide a natural explanation for the basic properties of these sources. The small thickness of the chromosphere above a spot is apparently associated with its low temperature as far as the layers where the density has already approached 10^9 cm^{-3}. This situation would require that the wave flux emanating from the photospheric spot layers be weakly dissipated in the chromosphere. A qualitative finding of weak wave dissipation in the chromosphere above a spot was obtained previously in [16].

2. A Model Radio Source

The spectra of radio sources and the wavelength dependence of the polarization in principle enable us to compute a model for a radio source. For these computations we shall adopt the radio-source spectra given in [1-3], taking the radio flux at $\lambda = 3$ cm as unit. These spectra are characterized by an approximately twofold rise in the radiant flux from $\lambda = 3$ cm to $\lambda = 5$ cm, and by a subsequent decline with increasing λ. The displacement of the maximum from $\lambda = 5$ cm to $\lambda = 10$ cm could be associated with an increasing source size toward longer wavelengths, or with an increasing contribution of floccular radiation during noneclipse observations [17]. In absolute value the flux of individual sources can differ by a factor of 3-5, because of the differing number of spots in a group and the differences in dimensions and physical conditions. In accordance with the Pulkovo observations we shall henceforth assume that at $\lambda = 3$ cm, $T_{eff} = 5 \cdot 10^5$ °K. For a source diameter $D_S = 17{,}000$ km this temperature would correspond to a flux $I_\lambda = 1.4 \cdot 10^{-22}$ W·m^{-2}·cps^{-1} (a source above a small group or a single spot).

The most important item for the model is the height dependence of the magnetic field. We shall assume that the spot field is represented by the

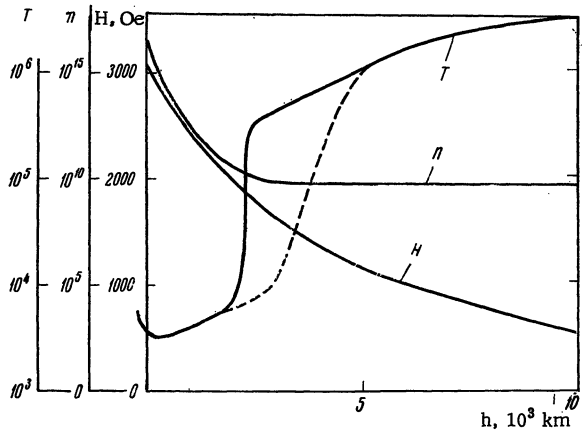

Fig. 1. Model atmosphere above a spot umbra.

field of a dipole located at 13,000 km depth. At the photospheric level this would correspond to a spot with a penumbral diameter $D \approx 37{,}000$ km and $H_{max} = 3100$ Oe. For particular spots the height dependence of the field may, of course, differ somewhat from that adopted here, although the qualitative picture should remain the same. The distribution of density with height will be taken as a hydrostatic distribution, extending from $n(0) = 2.5 \cdot 10^{16}$ cm^{-3} in the upper photosphere to $n = 5 \cdot 10^{9}$ cm^{-3} at $h \approx 3000$ km. The first value results from the fact that the gas pressures in spot and photosphere cannot be very different (see, for example, [18]), the second, from optical observations of coronal condensations, leading to $n = 10^{9}$–10^{10} cm^{-3}. In order for the hydrostatic distribution to yield so steep a decline in density in a short distance, the temperature in the chromosphere must hardly rise at all up to these heights, despite the low density. We shall adopt $T \approx 4000$ °K at the base of the chromosphere above the spot. The exact behavior of T and n at low heights is unimportant in our case.

From an analysis of the radio spectrum one can compute the function T(H), which for a known height dependence of the field will yield T(h). The appropriate formulas for magnetobremsstrahlung are given in [5]. In our case we must include the radiation for the second and third gyrofrequency harmonics. To simplify the computations we shall assume that the mean value of the angle between the field and the line of sight over the whole radio source is 30°. The characteristic dimension $L_H = \omega dl/d\omega_H$ for field variations is fairly small in our case ($L_H \approx 6 \cdot 10^{8}$ cm for $\lambda = 5$ cm and $h \approx 3000$ km); its height dependence between 3000 and 10,000 km can be neglected. The values for the optical thickness τ_{js} of a layer with given L_H (j = 1 for the extraordinary wave, j = 2 for the ordinary wave, and s is the number of the harmonic) will then be (n in cm^{-3}, T in °K):

$$\tau_{12} = 7.8 \cdot 10^{-13}\, nT, \quad \tau_{13} = 2.5 \cdot 10^{-22}\, nT^2,$$
$$\tau_{22} = 4.0 \cdot 10^{-15}\, nT, \quad \tau_{23} = 1.3 \cdot 10^{-24}\, nT^2.$$

Having τ_{js}, we can compute the combined flux of thermal radiation at a given frequency resulting from the contribution of both harmonics. By comparing the flux with the observed spectrum and polarization of the radiation, we can find the temperature T(H) corresponding to a given field strength. Although the method of trial and error used to allow for the simultaneous contribution of both harmonics is somewhat arbitrary, observations at several wavelengths would establish the T(H) relation, and hence T(h), fairly accurately. For example, if an appreciable drop in intensity (and a very high degree of polarization) occurs not at $\lambda \approx 2$ cm but at $\lambda \approx 3$ cm, then T(H) will change markedly (Fig. 1, dashed curve). The results of the computation are given in Table 1.

As a check, this model has been used to compute the radio flux for different λ and the polariza-

TABLE 1

s	H	τ_{1s}	τ_{2s}	T_e	T_{eff_1}	T_{eff_2}	$\overline{T}_{eff}$	I_λ	p
				$\lambda = 2$ cm					
2	2700	$\sim 3 \cdot 10^{3}$	~ 15	$3.6 \cdot 10^{3}$	$1.06 \cdot 10^{5}$	$3.6 \cdot 10^{3}$	$5 \cdot 10^{4}$	0.4	100%
3	1800	0,26	$1.3 \cdot 10^{-3}$	$3.2 \cdot 10^{5}$					
				$\lambda = 3$ cm					
2	1800	$2.5 \cdot 10^{3}$	12.5	$3.2 \cdot 10^{5}$	$5.8 \cdot 10^{5}$	$3.2 \cdot 10^{5}$	$4.5 \cdot 10^{5}$	1.4	30%
3	1200	1.02	$5 \cdot 10^{-3}$	$9 \cdot 10^{5}$					
				$\lambda = 5$ cm					
2	1070	$5.4 \cdot 10^{3}$	27	$1.35 \cdot 10^{6}$	$2.65 \cdot 10^{6}$	$1.35 \cdot 10^{6}$	$2 \cdot 10^{6}$	2.2	30%
3	713	8.8	$5 \cdot 10^{-2}$	$2.65 \cdot 10^{6}$					
				$\lambda = 10$ cm					
2	535	$1.3 \cdot 10^{4}$	66	$3.3 \cdot 10^{6}$	$4.0 \cdot 10^{6}$	$3.3 \cdot 10^{6}$	$3.65 \cdot 10^{6}$	1.0	10%
3	360	20	0.10	$4.0 \cdot 10^{6}$					

tion of the radiation (Table 1). The table includes the harmonic number s, the magnetic field H [Oe] at the level where the radiation is produced, as determined from the condition $\omega = s\omega_H = 1.76 \cdot 10^7 \cdot sH$, the optical thickness τ_{js} (j = 1 for the extraordinary, j = 2 for the ordinary wave), the kinetic temperature T_e at the level considered,

$$T_{\text{eff}_j} = \sum_{s=2}^{s} T_{js}(1 - e^{-\tau_{js}}), \qquad \overline{T}_{\text{eff}} = (T_{\text{eff}_1} + T_{\text{eff}_2})/2,$$

the radio flux $I\lambda$ [10^{-22} W·m^{-2}·cps^{-1}], assuming D_S = 17,000 km, and the degree of polarization $p = (T_{\text{eff}_1} - T_{\text{eff}_2})/(T_{\text{eff}_1} + T_{\text{eff}_2}) \cdot 100(\%)$. Figure 2 shows the relative radio spectra from the eclipse data (strong and weak sources [1]) and from observations with the large Pulkovo radio telescope [3]. A theoretical spectrum is also given in Fig. 2, as computed assuming a constant source size for different wavelengths. The spectrum agrees well with observations, although the computed flux at λ = 5-10 cm should evidently be increased because of the increased source size (see below). The computation indicates total polarization at λ = 2 cm, $p \approx 30\%$ at λ = 3-5 cm, and $p \approx 10\%$ at λ = 10 cm. However, the value for λ = 3 cm is found to be very sensitive to the model adopted, and for the distribution T(h) shown by the dashed curve in Fig. 1, p = 100% for λ = 3 cm. These results agree with the polarization observations [1, 2, 4].

On our model a radio source is represented by an extended plane region ≈20,000 km in diameter and several thousand kilometers thick. Because of changes in the projected source area the radio emission should vary $\sim\cos\theta$, in agreement with observation [5]. If the source were located at a great height and had a disordered magnetic field and a thickness comparable with its diameter, then the $\cos\theta$ variation would be absent.

The law $I \sim \cos\theta$ breaks down for $\theta \approx 90°$. The reason is that at the limb the role of the magneto-bremsstrahlung mechanism diminishes, and bremsstrahlung from coronal condensations is apparently observed. Adopting $n = 5 \cdot 10^9 e^{-h/h_0}$, where $h_0 = kT/mg = 4.3 \cdot 10^9$ cm, $T = 2.5 \cdot 10^6$ °K, and $L \approx 10^{10}$ cm, we obtain for λ = 5 cm a temperature $T_{\text{eff}} \approx T_\tau = 2.5 \cdot 10^6 \cdot 0.025 \approx 6 \cdot 10^4$ °K. For the bremsstrahlung mechanism the spectrum of limb sources should be flat for λ = 1-20 cm, and the polarization should be weak.

The eclipse observations exhibit a sharp decline in radiant flux at the edges of the sources [4]. This sharp boundary occurs because with increasing distance from the source axis the formation levels of the working harmonics sink downward, following the magnetic-field isolines. Near the spot axis dH/dh is small, the formation levels remain at T ≈ const, and the radiant intensity suffers little variation. As the formation levels emerge into the region of strong temperature gradient, a sharp decline in the radio-emission intensity sets in. To explain this intensity decline by a field variation alone, one would have to assume a sharp cutoff in the field at the boundary of the emitting region, which seems improbable from certain experimental and theoretical considerations.

Thus the mere presence of a sharp boundary provides further evidence for the existence of a region with a large temperature gradient in the radio source.

These considerations also furnish an independent estimate, within the scope of our model, for the dimensions of the radio-emitting region. For a single spot and for $\alpha = 30°$, we obtain the following values: D ≤ 10,000 km for $\lambda \leq 3$ cm, D ≈ 16,000 km for λ = 5 cm, and D ≈ 23,000 km for λ = 10 cm. Since this result depends materially on our adopted idealization for the spot field (possibly the field varies more smoothly near the axis), the strong increase we have found in the source size with λ is somewhat exaggerated. In particular, for $\lambda \leq 3$ cm only an upper estimate on the size is obtained. However, the dimensions of the source actually should increase for λ = 3-10 cm, and as radio-telescope resolutions improve this effect will probably be detected.

The increase in source size with λ allows us to increase somewhat our computed values for the

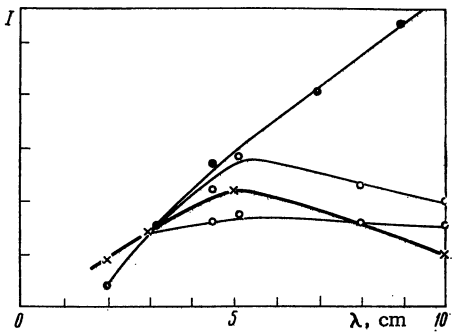

Fig. 2. Radio spectrum of sources above spots. Dots, observations with the large Pulkovo radio telescope; circles, eclipse data; thick curve, spectrum computed from the model, assuming a constant source diameter for different λ. For each spectrum the radiant flux at λ = 3 cm is adopted as unit.

radio flux at 5-10 cm with respect to the 3-cm flux. In the same manner we can explain the slight displacement in the maximum of the spectrum in the region of longer wavelengths. However, there would hardly be any point in making a detailed comparison of the theoretical spectrum with any of the observed spectra, in view of the indefiniteness of the observations and the semiqualitative character of our proposed model.

The source dimensions derived above correspond to the sizes of spot umbrae, in accord with the polarization observations [4]. For sources located above spot groups the combined flux corresponds to a diameter $D \approx 70{,}000$ km at $\lambda \approx 7$ cm ($I_\lambda \approx (30\text{-}35) \cdot 10^{-22}$ W·m^{-2}·cps^{-1}); for faint sources the dimensions at $\lambda = 7$ cm practically coincide with the values we have obtained.

3. Heating of Chromosphere and Corona above a Spot

Heating of the chromosphere occurs through dissipation of the energy of weak shock waves. In a magnetized plasma these waves comprise accelerated and retarded modes. The energy flux varies with height both through dissipation and because of refraction and reflection of waves, with violation of the conditions of geometric optics. This situation creates difficulties. For example, in an active region accelerated waves are primarily formed, but they are strongly reflected and cannot account for the heating of the upper chromospheric layers [19]. This difficulty is removed if one considers the interaction of waves and their transformation from one type to another [20]. The transformation is most efficient in layers where the velocities are comparable, that is, where $V_A \approx V_S$.

The generation of waves from a spot region and their dissipation above a spot have been treated in [16, 21]. It has been shown that in the upper layers of the convective zone under a spot, Alfvén and retarded waves are primarily formed. With allowance for reflection, the value $\pi F \approx 3 \cdot 10^8$ ergs/cm^{-2}·sec^{-1} has been obtained for the flux emerging from a large spot. This estimate has shown that for H = 2000-3000 Oe the dissipation in the chromosphere is smaller than in active and undisturbed regions, and that a large Alfvén-wave flux escapes into the corona. The estimate utilized a model for the undisturbed chromosphere, since a model for the region above a spot had not yet been computed.

Let us consider the propagation of waves above a spot. In the interaction region below the photosphere, where $V_A \approx V_S$, the energy should be redistributed, since all three types of wave emerge from the spot. The mean period for these waves should be no less than 10^3 sec, since the wave-generation layer lies deeper than the layer responsible for the granulation [21]. With this period the wavelength of the sound and particularly the Alfvén waves will considerably exceed the scale height, so that the waves in general cannot be considered harmonic.

We shall now examine the propagation of each type of wave. The sound waves move along H and are already weak discontinuities when they emerge into the chromosphere. Their amplitude increases with height so long as the gas velocity V remains below the sound velocity V_S. As V approaches V_S the dissipation increases sharply, and we may subsequently take $V = V_S$. The energy flux of the waves will then be

$$\pi F = \alpha \rho V^2 V_S = \alpha \cdot 1.7 m_H n V_S^3, \qquad (1)$$

where α is the mean volume occupied by the gas moving in the wave relative to the entire volume of a column of the chromosphere. Since the period is long and the waves follow each other at intervals of more than 10^3 sec, the value of α should be less than 0.1. The coefficient 1.7 characterizes the contribution of He and other elements to the value of the density.

Since the model considered has a temperature nearly constant to the transition region, $V_S = \text{const}$ and reflection of sound waves will not take place. The flux will therefore vary because of dissipation alone, and we may write for the dissipation (per cm^3) the equation

$$E_d = -\frac{d\pi F}{dh} = -\frac{d\pi F}{dn}\frac{dn}{dh} = \alpha \cdot 1.7 m_H V_S^3 n h_0^{-1}$$

$$= \alpha \cdot 1.7 m_H^{1/2} \gamma^{3/2} g (kT)^{1/2} n. \qquad (2)$$

Here we have used the equations for V_S and h_0. The quantity γ is the adiabatic index. Equation (2) gives E_d directly for a level with prescribed n, if the wave amplitude is not small there. Taking T = 5000 °K and $\alpha < 0.1$, we find for the level with $n = 10^{10}$ cm^{-3} a value $E_d < 10^{-4}$ erg/cm^{-3}·sec^{-1}. For $n = 10^{11}$ cm^{-3}, the upper bound on E_d is one order greater. The radiation of the upper chromosphere ($n = 10^{10}$-10^{11} cm^{-3}) amounts to $2\pi F/l \approx 2 \cdot 10^6/2 \cdot 10^8 = 10^{-2}$ erg/cm^{-3}·sec^{-1} [20, 21], which is another order greater than this upper bound. Thus dissipation of sound waves cannot substantially raise the temperature of the chromosphere, and our assumption of an isothermal chromosphere is supported.

Alfvén waves will experience strong reflection; their flux $\pi F \sim \rho^{1/2}$. Although one cannot speak of regular reflection here, since the wavelength considerably exceeds the thickness of the chromosphere, the physical meaning of reflection in this case is that the lines of force will travel, preserving their shape, so that the gas velocity $V \approx$ const. The energy density will then decline rapidly with height and, as can readily be estimated, will be insufficient to heat the chromosphere.

Accelerated waves should also experience strong reflection. Here, however, the motions will have a more complex character, and the reflection law has not been investigated for the conditions of a thin layer. The dissipation of these waves under chromospheric conditions is small in any event, but to explain coronal condensation we would have to assume that about 1% of the flux emanating from a spot penetrates into the corona. The accelerated waves will not be dissipated in the corona either, but at heights $h \gtrsim 100{,}000$ km the field weakens so much in our model that $V_A \approx V_S$. Dissipation will then be enhanced; moreover, some of the energy will be transformed into retarded waves, which will also dissipate, becoming weak shock waves. Thus a qualitative model, which so far is difficult to confirm by quantitative computation, could be described as follows. Part of the energy in the waves emanating from a spot would penetrate to the intermediate coronal layers and dissipate there. Energy will thence be transported by thermal conductivity into lower coronal layers—into a coronal condensation. This process will set up the small temperature gradient in the corona that is needed to explain the polarization at longer wavelengths.

Let us estimate the value of the mean temperature gradient in the corona. The radiation of a coronal condensation (primarily in the x-ray region) amounts to about $2 \cdot 10^6$ ergs/cm$^{-2} \cdot$ sec^{-1} [22, 23]. This energy is radiated primarily by the low, dense layers, and then enters the upper layers. It should therefore be transported by thermal conduction. The conductivity coefficient $\varkappa = 2 \cdot 10^{-6} T^{5/2}$ [24]. Hence

$$Q = \varkappa \nabla T = 2 \cdot 10^{-6} T^{5/2} \nabla T = 2 \cdot 10^6. \quad (3)$$

Setting $T = 2 \cdot 10^6$ °K and $\nabla T = \Delta T / l$, we have $\Delta T / l \sim 2 \cdot 10^{-4}$, which for $l = 5 \cdot 10^9$ cm (a condensation as described in [25]) yields $\Delta T = 10^6$ °K. This would explain why the corona above spots radiates in the green line, but at the top of the tube, coupled to a spot, in the yellow line, corresponding to a higher temperature [25].

The authors are grateful to G. B. Gel'freikh and E. Ya. Zlotnik for valuable discussions of several topics treated in the paper.

LITERATURE CITED

1. A. P. Molchanov, Izv. Glav. Astron. Obs. Pulkove, 24, No. 1, 38 (1964).
2. G. Swarup et al., Astrophys, J., 137, 1251 (1963).
3. Sh. B. Akhmedov et al., Solnech. Dannye, No. 2, 62 (1966).
4. D. V. Korol'kov, N. S. Soboleva, and G. B. Gel'freikh, Izv. Glav. Astron. Obs. Pulkove, 21, No. 5, 81 (1960).
5. V. V. Zheleznyakov, Radio Emission of the Sun and Planets [in Russian], Moscow, Nauka (1964); V. V. Zheleznyakov, Astron. Zh., 39, 5 (1962) [Soviet Astronomy—AJ, Vol. 6, p. 3].
6. V. N. Ikhsanova, Izv. Glav. Astron. Obs. Pulkove, 21, No. 5, 62 (1960).
7. A. S. Grebinskii and A. P. Molchanov, Geomagnetizm i Aéronom., 4, 635 (1964).
8. G. F. Hale and S. B. Nicholson, Magnetic Observ. of Sunspots 1917-1924, Carnegie Inst. of Washington (1938).
9. É. A. Baranovskii and V. E. Stepanov, Izv. Krym. Astrofiz. Obs., 18, 66 (1958).
10. A. B. Severnyi and V. Bumba, Observatory, 78, No. 902, 33 (1958).
11. B. Ioshpa, E. I. Mogilevsky, and V. N. Obridko, Space Research, (Amsterdam, North-Holland), 4, 789 (1963).
12. J. C. Henoux, Comt. Rend. Acad. Sci. France, 26, 159 (1963).
13. M. Adam, Monthly Notices Roy. Astron. Soc., 126, 135 (1963).
14. A. B. Severnyi, Izv. Krym. Astrofiz. Obs., 33, 34 (1965).
15. B. A. Ioshpa and V. N. Obridko, Solnech. Dannye, No. 3, 54 (1965).
16. M. Marik, Candidate's dissertation [in Russian], Moscow, Shternberg Astron. Inst. (1966).
17. A. R. Abbasov, Vestnik Leningr. Gos. Univ., No. 1, 174 (1966); A. R. Abbasov, Sh. Akhmedov, A. S. Grebinskii and A. P. Molchanov, Astron. Zh. (1967) (in press).
18. Cl. Van't Veer Menneret and F. Van't Veer, Ann. Astrophys., 28, 1026 (1965).
19. D. E. Osterbrock, Astrophys. J., 134, 347 (1961).
20. S. B. Pikel'ner and M. A. Livshits, Astron. Zh., 41, 1007 (1964) [Soviet Astronomy—AJ, Vol. 8, p. 808].
21. M. Marik, Astron. Zh., 43, 400 (1966) [Soviet Astronomy—AJ, Vol. 10, p. 315].
22. M. A. Livshits, Astron. Zh., 41, 473 (1964) [Soviet Astronomy—AJ, Vol. 8, p. 376].
23. G. S. Ivanov-Kholodnyi, Geomagnetizm i Aéronom., 5, 705 (1965).
24. L. Oster, Zs. Astrophys., 42, 228 (1957).
25. M. K. Aly, J. W. Ewans, and F. Q. Orrall, Astrophys. J., 136, 956 (1962).